European Battery, Hybrid and Fuel Cell Electric Vehicle Congress
Geneva, 14th - 16th March 2017

A Compensation Method for Production Tolerances in Electric Drive Systems Using an Extended Open-Loop Torque Control

Markus Ott[1], Alexander Beckmann[1], Prof. Dr.-Ing. Joachim Böcker[2]
[1]*Daimler AG, Power Electronics Software Development, markus.o.ott@daimler.com*
[2]*Paderborn University, Power Electronics and Electrical Drives, boecker@lea.upb.de*

Abstract

Interior permanent magnet synchronous machines are unavoidably subject to production tolerances. Quantities like permanent magnet flux or air gap thickness of a machine may deviate with regard to their nominal parameter values. Driven with a conventional torque control strategy this leads to inaccuracy of the output torque. Especially for traction drives in road vehicles, significant torque error is not acceptable. In this paper, a method for compensation of such deviations is presented. It is based on maximum-torque-per-current (MTPC) open-loop torque control. The conventional torque controller is doubled leading to a Parallel Torque Compensation (PTC) structure. It is capable of adapting to an individual machine increasing torque accuracy and efficiency. The concept is proven by simulation as well as test bench measurements with an exemplary machine, showing a significant improvement of torque accuracy with the error reduced from 12 % to 2 % with respect to maximum torque. At the same time, the maximum torque available is increased. With PTC, a purely software-based solution is given that optimizes torque accuracy and efficiency in permanent magnet synchonous drives.

Keywords: Permanent magnet motor, Automotive traction application, Production Tolerance, Torque control

1 Introduction

Torque accuracy is important for automotive traction drives. Controlling torque precisely ensures the delivery of the specified power. This is important for road approval and for customer satisfaction. For some applications, e.g. for torque vectoring, the precise torque tracking of two independent machines must be ensured. For hybrid vehicles, the exact knowledge of the produced torque is important for coordinating the electrical machine and the combustion engine. For hybrid and electric vehicles, inverter-fed interior permanent magnet synchronous machines (IPMSM) are widely used. No torque sensor is available in the vehicle due to technological challenges and its high cost. Torque is therefore controlled without feedback, solely based on the knowledge of reference machine parameters. A torque tracking accuracy with an error of 1-2 % with respect to maximum torque can be achieved, assuming that the parameters of the individual machine are known. At the same time, production tolerances unavoidably lead to deviations of torque and power. Obviously, the average torque accuracy will deteriorate, if all mass produced machines are operated with the same controller based on the nominal data. Therefore, research focuses on the causes and the effects of such deviations in PMSM [1, 2, 3, 4, 5].

The knowledge about the effects of manufacturing tolerances can be used in various ways: First, detected correlations help to define reasonable tolerance bands in the design stage of a machine. Second, by knowing about the effects with the highest impact the manufacturing process can be

optimized, i.e. by selective rotor assembly [6]. Third, methods for control-related compensation can be developed to increase torque accuracy, which is the scope of this paper. It allows to define wider component tolerances and thus to reduce cost without effecting torque accuracy.
In literature, there are a few papers on control-related compensation methods for manufacturing tolerances. One approach is online parameter adjustment [7]. For its implementation, phase voltage is used that is not measured in most automotive inverters. It has to be estimated from DC-voltage measurements and pulse-width modulation. Unfortunately, the voltage estimation requires very good knowledge about the semiconductors in the inverter and depends on their manufacturing tolerances. Moreover, there are papers presenting compensation techniques in a different context: The effects of temperature are similar to the effects of manufacturing tolerances in the magnets of a PMSM – both affect the permanent magnet flux [8, 9].
In this paper, the idea of a compensation for deviations of permanent magnet flux and air gap width is used. In their previous work the authors showed the dominant effect of these influence factors [5]. An offline identification is introduced to evaluate the deviation of an individual machine from its reference. The information gained from these measurements can be used for compensation. Following this method, the saturation effects in the machine are taken into account. The impact of the deviations on system efficiency is considered.

2 Conventional open-loop torque control

All investigations are based on detailed information about the nonlinear flux linkages of direct axis $\psi_d(i_d, i_q)$ and quadrature axis $\psi_q(i_d, i_q)$ and their absolute value $\psi(i_d, i_q)$ according to (1).

$$\psi = \sqrt{\psi_d^2 + \psi_q^2}. \quad (1)$$

$$T = \frac{3}{2} p \left(\psi_d(i_d, i_q)\, i_q - \psi_q(i_d, i_q)\, i_d\right) \quad (2)$$

The flux linkages are independent of the rotational speed of the machine. They can either be gained by Finite Element Analysis (FEA) or by dynamometer (dyno) measurement and be stored in look-up-tables (LUT) with respect to i_d and i_q. Moreover, the fixed relationship between the applied phase current in the machine and the respective output torque is given with the number of pole pairs p in (2). Both values are shown in Fig. 2a as isolines, absolute flux linkage $\psi(i_d, i_q)$ with its typical elliptic shape and torque $T(i_d, i_q)$.

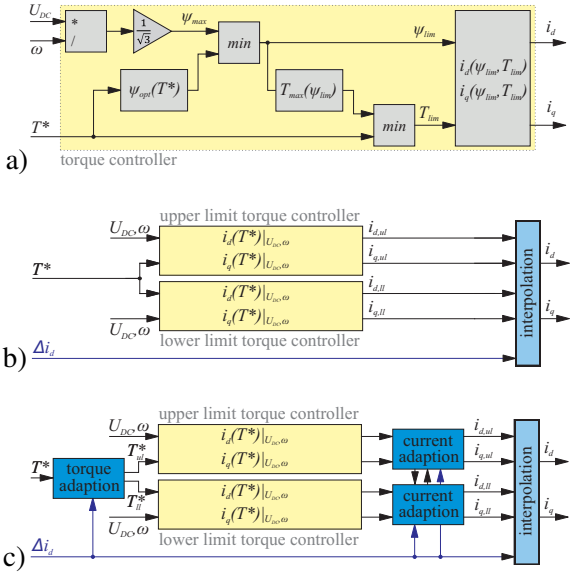

Figure 1: Open-loop torque control based on MTPC operation strategy. a) conventional structure [10], b) simple sPTC structure, c) extended PTC structure

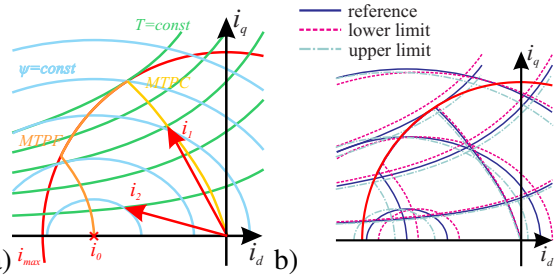

Figure 2: Absolute flux linkage $\psi(i_d, i_q)$, torque $T(i_d, i_q)$ and the operating limits of the MTPC control scheme. a) for a reference machine with labeling, b) these lines again for the reference machine and for an upper and lower limit sample.

The control strategy can be derived from these machine characteristics. There are two constraints that limit the operation area: The current is mainly restricted by thermal limits of machine and inverter. Its limit i_{max} is shown as a red circle in Fig. 2. The maximum absolute flux linkage in the machine is restricted by the DC-link voltage U_{DC} and the rotational speed ω by

$$\psi_{max}(\omega) = \frac{U_{DC}}{\sqrt{3}\omega}. \quad (3)$$

This maximum flux linkage $\psi_{max}(\omega)$ can be visualized as one of the flux isolines in Fig. 2. Therefore, the operation area of the machine is physically restricted to all operation points enclosed by the i_{max}-circle and the respective $\psi_{max}(\omega)$-ellipse.

2.1 Torque control

For this paper, an MTPC (maximum-torque-per-current) open-loop torque control strategy is used in the inverter software. It is briefly explained in the following, more details are in [10]. The control strategy ensures a ohmic loss-minimal operation of the machine by minimizing the amplitude of the current while keeping the operation limits. As any i_d/i_q-combination along one torque isoline in Fig. 2 leads to the same torque, the combination with the smallest absolute current is chosen (i.e. the current vector $\boldsymbol{i}_1$). Calculating this optimum current point for each torque results in the optimal MTPC line shown in Fig. 2. According to (3), the limiting flux ellipse is large at low speed and all points on the MTPC line are valid operation points. Therefore, for low speeds MTPC points are always chosen.

For speeds above rated speed, the $\psi_{max}(\omega)$-ellipse excludes some points of the MTPC line. Small torque values on the MTPC line may still be located inside the allowed area while large torque values are outside. To reach these large torque values, additional field weakening d-axis current i_d can be used. The current vector $\boldsymbol{i}_2$ in Fig. 2 is an example for an operation point at higher speed. The i_d/i_q-combination of the intersection point of the commanded torque line and the limiting flux line will be chosen.

The maximum available torque for a given speed is then the one at the intersection of the corresponding i_{max}-circle and $\psi_{max}(\omega)$-ellipse. This defines the upper part of the MTPF (maximum-torque-per-flux) line (Fig. 2a). For each flux ellipse, there is one point where the torque is at its maximum and its tangent is parallel to the tangents of the torque lines. These points mark the lower part of the MTPF line. The MTPF line therefore represents the line, along which for a given maximum flux $\psi_{max}(\omega)$, restricted by (3), the maximum torque can be reached.

To sum up, the area between MPTC and MTPF lines is the optimal operating area for the IPMSM. If the voltage limit allows, points on the MTPC line are chosen. If limited by the voltage limit, additional negative i_d-current up to the MTPF line can be used to reach higher torque.

2.2 Implementation of torque control

This control strategy can be implemented in the inverter software with the structure shown in Fig. 1a. Four offline calculated look-up-tables (LUTs) are used, as the interrelations in the machine are too complex for an online calculation in an automotive controller. The commanded torque T^* is fed into the first LUT $\psi_{opt}(T^*)$. The result is the flux ψ_{opt} that is necessary to operate the machine at the MTPC for the commanded T^*. This flux ψ_{opt} is then compared to the limiting flux ψ_{max} according to (3) by

$$\psi_{lim} = \min(\psi_{opt}, \psi_{max}). \tag{4}$$

For low speed, $\psi_{opt} < \psi_{max}$ is valid and therefore $\psi_{lim} = \psi_{opt}$. For higher speed when voltage limits the operation on MTPC, $\psi_{opt} > \psi_{max}$ and therefore $\psi_{lim} = \psi_{max}$ from (4). The LUT $T_{max}(\psi_{lim})$ determines the torque at the MTPF for a given flux value ψ_{lim}. As mentioned before, this is the maximum available torque for the given flux and the commanded torque gets limited by

$$T_{lim} = \min(T_{max}(\psi_{lim}), T^*) \tag{5}$$

to T_{max}. The values T_{lim} and ψ_{lim} are then fed into two LUTs $i_d(\psi_{lim}, T_{lim})$ and $i_q(\psi_{lim}, T_{lim})$. These LUTs are the inversion of the fuctions $\psi(i_d,i_q)$ and $T(i_d,i_q)$ from (1) and (2) displayed in Fig. 2. They are used to determine the according current vector. Using this current vector to drive the machine will exactly produce the commanded torque T^* – without any torque feedback.

3 Compensation method

In Section 2 the standard approach for open-loop torque control is described. A machine is characterized to gain the flux linkages $\psi_d(i_d, i_q)$ and $\psi_q(i_d, i_q)$. With the flux linkages, LUTs for the inverter software are generated. These LUTs are then used to drive the machine. It will produce the commanded torque with the shortest current vector possible.

Conventionally, the mentioned LUTs are derived from the flux characteristics of one reference machine in the development phase of a drive. They are then used for all machines that are produced. Applying this exact torque control structure to an individual machine with deviations due to manufacturing tolerances will lead to errors in torque.

3.1 Torque errors resulting from parameter deviations

The effect of permanent magnet flux and air gap deviation on flux linkage in the machine is derived in previous work [5]. The flux linkage characteristic $\psi_{ref}(i_d, i_q)$ of a reference machine (denoted by the index '*ref*') with nominal design parameters is shown in Fig. 3a. The characteristic is computed with Finite Element Analysis (FEA) based on the machines nominal design parameters. For an individual deviating machine with a permanent magnet flux increased by 5 % the flux table $\psi_{ind}(i_d, i_q)$ in Fig. 3a (index '*ind*' for 'individual') are obtained. With (2) the torque characteristics can be derived (Fig. 3b). In Fig. 3c the torque error is visualized. For a permanent

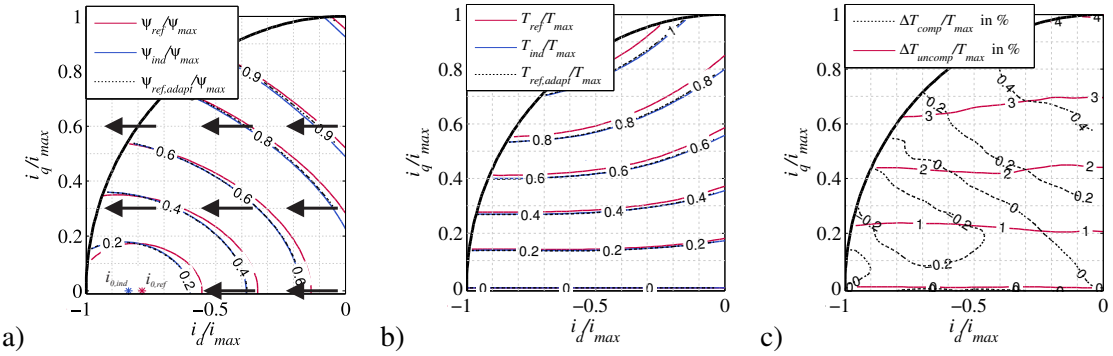

Figure 3: Comparison of the reference machine (red) and the individual machine with increased *permanent magnet flux* (blue). The black dotted lines indicate the values with compensation. a) absolute value of the flux ψ, b) resulting torque T for each machine, c) difference $\Delta T_{uncomp} = T_{ind} - T_{ref}$ and $\Delta T_{comp} = T_{ind} - T_{ref,adapt}$.

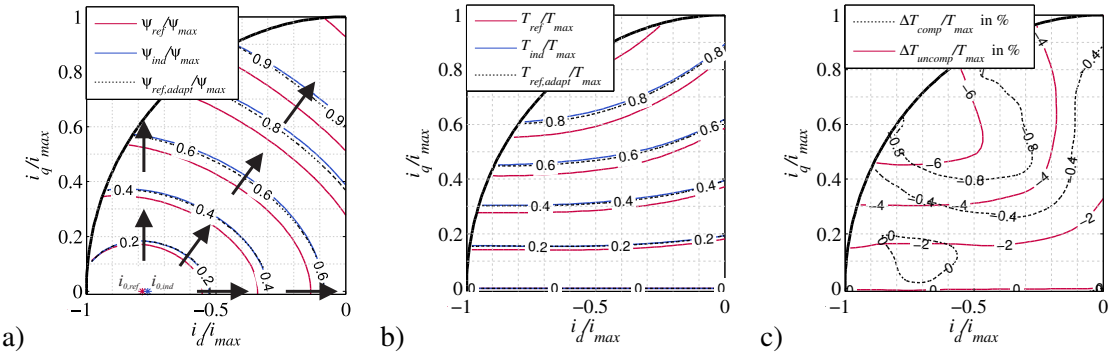

Figure 4: Comparison of the reference machine (red) and the individual machine with larger *air gap* (blue). The black dotted lines indicate the values with compensation. a) absolute value of the flux ψ, b) resulting torque T for each machine, c) difference ΔT_{uncomp} and ΔT_{comp}.

magnet deviation of 5 %, the torque error is up to 4 % with respect to maximum torque T_{max} for an exemplary IPMSM. The main effect that can be observed is a shifting of the flux isolines along the d-axis as indicated by the arrows in Fig. 3 [5]. The main reason is that flux resulting from d-axis current and permanent magnet flux are pointing in the same direction – and therefore influence each other. A deviation of the air gap dominantly influences the inductances in the machine and therefore affect both, ψ_d and ψ_q. It leads to a scaling effect in the flux linkage characteristic that is visible in d- and in q-axis (Fig. 4). As is shown in the figure, a reduction of the air gap width of 30 % leads to torque error of more than 7 %.

3.2 Principle of compensation

With this understanding of the underlying effects, two steps are necessary for successful compensation: The first step is to detect the deviations in an individual machine. As showed in [5], this can be done by measuring the short-circuit current and the open-circuit voltage at the end of production line. The short-circuit current i_{sc} indicates the center point of the flux-ellipses in Fig. 3 and Fig. 4 where the flux linkage in the machine is zero. It produces evidence on how much the flux isolines are shifted along the d-axis. The open-circuit voltage v_{oc} is proportional to the flux linkage in the origin of the i_d/i_q-plane and gives a good indication on the scaling of the flux isolines. These two tests at the end of production give enough information on how to apply the compensation on an individual machine.

The second step is the compensation itself. To compensate for tolerance effects, the LUTs used in the inverter software (based on the characteristics of the reference machine) have to be adjusted to fit the flux characteristics of the individual machine. The measurements of v_{oc} and i_{sc} of both machines can be used. The flux isolines of the reference machine can be altered in such way that the flux at the origin and the flux an the center point of the flux-ellipses is congruent to the deviating machine. For permanent magnet flux deviation the adjustment is a shift along the d-axis with a slight scale in q-axis [5]. The adapted tables then fit the flux lines of the individual machine ψ_{ind} very well. Consequently, the mismatch between torque $T_{ref,adapt}$ calculated on

these adapted isolines $\psi_{ref,adapt}$ and torque T_{ind} of the machine with the deviations is significantly reduced (Fig. 3b and c). Starting without compensation from a torque error of over 4 %, it can be reduced to less than 0.4 %. As all percentage figures in the paper, this is with respect to maximum torque. Applying the same principle for air gap deviation (Fig. 4), torque error can also be significantly reduced from 7 % to 1 % by compensation.

3.3 Simple Parallel Torque Compensation (sPTC)

For using the compensation principles online in a vehicle, they have to be transferred into executable algorithms. Considering the effects of deviations with the open-loop torque control according to Section 2.2 would require to adapt its LUTs. Due to their complexity this cannot be done easily online during runtime. Another option would be to prepare multiple datasets during development and to chose the dataset that is closest to the individual machine before flashing the device in the vehicle. A drawback is the logistical effort during production of the system and that no dynamical changes during runtime are possible. Therefore, a method is proposed in this paper that implements the compensation principle in a parallel open-loop torque control scheme.

To start with, only the compensation for the permanent magnet flux deviation is described. Limit sample machines and their characteristics are used in the following. They are machines intentionally modified to represent the upper and lower bound of the tolerance band. The characteristics of both limit samples and of the reference machine are calculated with FEA. In Fig. 5a, an upper limit sample for magnets with a deviation of $+5$ % in its magnets remanence field density is simulated with the conventional open-loop control of the reference machine. It shows the maximum torque error of $+3.9$ % to be expected without compensation.

To overcome this error, the idea is doubling the open-loop control structure of Fig. 1a as shown in Fig. 1b. With the two calculations in parallel, the structure is called simple Parallel Torque Control (sPTC). The LUTs in the two separate torque control structures are calculated from the flux characteristics of an upper and a lower limit sample machine respectively. These characteristics can be gained by two ways: One way is building dedicated limit samples for the machine type under development – then the characteristics can simply be measured and used in the LUTs. Another way is using the investigations shown above in Section 3.1 to derive the limit samples' characteristics from their reference machine. For the simulations in this paper, the characteristics of limit sample machines are gained from FEA calculations. The characteristics and the corresponding operation limits for an upper and lower limit sample as well as for the reference machine are shown in Fig. 2b.

Either way, both open-loop torque control structures calculate one pair of i_d/i_q-currents, each fitting the corresponding limit sample machine ($i_{d,ul}$/$i_{q,ul}$ for the upper limit and $i_{d,ll}$/$i_{q,ll}$ for the lower limit). To drive any individual machine, its position a between the limit samples has to be determined.

This can be quantified based on the short-circuit current of the individual machine $i_{sc,ind}$ to the short-circuit currents of the upper and lower limit machine $i_{sc,ul}$ and $i_{sc,ll}$:

$$a = \frac{i_{sc,ind} - i_{sc,ll}}{i_{sc,ul} - i_{sc,ll}} \tag{6}$$

Then, these two pairs of currents can be interpolated accordingly by

$$i_d = a\, i_{d,ul} + (1-a)\, i_{d,ll} \qquad a \in [0,1]. \tag{7}$$

$$i_q = a\, i_{q,ul} + (1-a)\, i_{q,ll} \tag{8}$$

For example, for driving the upper limit sample, $a = 1$ would be chosen and for the lower limit sample, $a = 0$ would be valid. Assuming a symmetric tolerance band, the reference machine would be exactly in the center of the two limit samples with $a = 0.5$.

Using sPTC, the calculated currents fit exactly for the limit samples. Driving a limit sample with sPTC therefore always leads to zero torque error. For any individual machine in between, the currents are not exactly correct. Still, torque accuracy is increased as can be seen comparing Fig. 5a and b. In Fig. 5b, sPTC is applied to a reference machine. FEA calculated characteristics of upper and lower limit samples are used in the controller according to 1b with $a = 0.5$. Driving the reference machine in the center of the tolerance band with $a = 0.5$ represents the worst case concerning torque accuracy. Still, with sPTC the torque error is reduced from 3.9 % in Fig. 1a to below 1 % for most points.

However, although this is already a large improvement compared to Fig. 5a, it still clearly shows areas with significant torque error up to a maximum of 1.5 % at the upper MTPF. The deviations boil down to three main effects that will be discussed in the following. Three extensions are added to the structure in Fig. 1b finally leading to Fig. 1c.

3.4 Extension 1: Adaption of the commanded torque

One general problem exists in the whole driving range: for increasing torque command, an almost linear increase in torque error is visible.

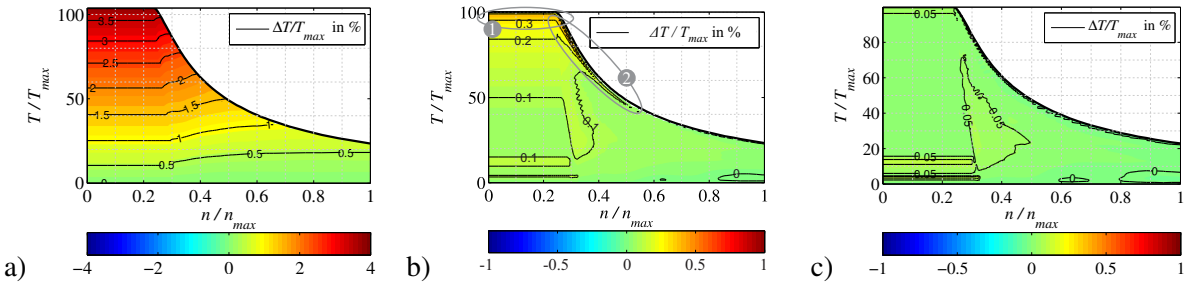

Figure 5: Simulated torque accuracy in the torque-speed-plane: a) without any compensation, b) with simplePTC, c) with the final PTC. Torque error $\Delta T = T_{sim} - T^*$ is calculated from the output torque of the simulated individual machine T_{sim} and the commanded torque T^*.

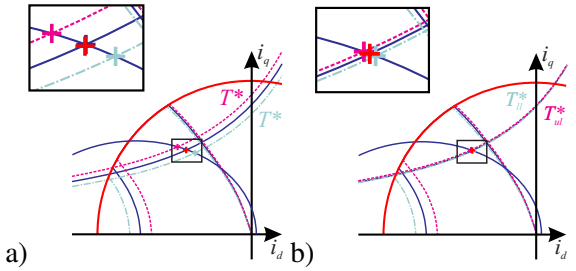

Figure 6: Extension 1: a) for upper and lower limit samples, the same torque command is reached on different torque isolines and interpolation leads to linearization error. b) by adapting the commanded torque, the respective isolines are closer together and the linearization error is reduced.

Consider the torque isolines in Fig. 6a, marking the same torque level for three different machines: the reference machine and the limit samples. Assume a certain torque command, i.e. $T/T_{max} = 0.5$. Feeding this command into the two seperate torque controllers, each delivers its i_d/i_q-points on the according isoline indicated by the corresponding marker in Fig. 6a. The isoline for the upper limit sample is at lower currents compared to the one for the lower limit sample – for a machine with stronger magnets, less current is needed to get the same amount of torque. The higher the commanded torque, the farther apart are the isolines and the determined i_d/i_q-points. These points then are interpolated linearly according to (7) and (**??**)current-interp2:. As the flux and torque characteristics are nonlinear, this leads to lineralization-errors. This can be seen looking at the markers in Fig. 6a. The ideal point for the torque command in the reference machine is the intersection of the blue flux ellipse and the blue torque isoline, marked by the blue marker. With the linear interpolation, the red marker is calculated which is not exactly at the same position as the blue marker.

To avoid this effect, the torque command for the torque controllers is modified according to the measured short circuit currents (visualized by the block "torque adaption" in Fig. 1c). For the upper limit torque controller, torque command is increased and for the lower limit torque controller, it is decreased:

$$T^*_{ll} = \frac{i_{sc,ll}}{i_{sc,ind}} T^* \tag{9}$$

$$T^*_{ul} = \frac{i_{sc,ul}}{i_{sc,ind}} T^*. \tag{10}$$

Therewith, the torque isolines of T^*_{ll} and T^*_{ul} for their respective characteristics lead to i_d/i_q-points that are closer to each other (Fig. 6b). Interpolating linearly between the two gives more accurate results – in Fig. 6b, the blue and the red marker are congruent.

3.5 Extension 2: Extension of LUT for lower limit

A second area of larger torque error is just below maximum torque marked with the number 1 in Fig. 5b. In the i_d/i_q-plane shown in Fig. 7 this is the area where the MTPF line follows the current limit circle. The reason is the different maximum torque of upper and lower limit sample for a given speed at the current limit. This current limit is implicitly included in the LUTs of the torque controllers. Assume a commanded torque of $T^*/T_{max} = 0.99$ for a reference machine. In Fig. 7a the torque isolines for upper and lower limit sample as well as for the reference machine are depicted. For a given commanded torque, again the intersection of torque isoline and, if above rated speed, limiting flux ellipse has to be chosen. For the upper limit and the reference characteristics the commanded torque is *inside* their current limits. Meanwhile, for the lower limit sample it is *outside* the limits. For the lower limit sample, therefore no intersection point can be found as it is restricted to the maximum current i_{max}. Consequently, the calculated $i_{d,ll}/i_{q,ll}$-point of the lower limit torque controller is on the maximum current circle (displayed by the marker at Fig. 7a). Using this

point for interpolation with (7) gives the point in between the markers of upper and lower torque controllers (interpolated point indicated by red marker). This point does not lead to the correct torque in the reference machine (which is the intersection point of the reference machines isolines, indicated by blue marker on the blue solid line).
One possible solution for this problem is to virtually extend the current limit for the lower limit torque controller as shown in Fig. 7b. For the same request of $T^*/T_{max} = 0.99$, the $i_{d,ll}/i_{q,ll}$-point of the lower limit torque controller is no longer restricted. Using this point for interpolation will lead to a correct torque in the reference machine.
The drawback of this solution is that the current limit is not considered implicitly, as the calculated current points of the lower limit torque controller can be outside the actual current limit. Let us assume a torque request of $T^*/T_{max} = 1.01$. A conventional torque controller (Section 2) would limit the request to $T^*/T_{max} = 1.0$ by implicitly keeping the current limit. With PTC and the extended current limit, the interpolated i_d/i_q-point is outside the physical current boundary i_{max}. One solution is comparing the interpolated i_d/i_q-current to the limit i_{max}. If the interpolated point is found to be outside the limits, the $i_{d,ll}/i_{q,ll}$-point must be adjusted. It must be ensured that the interpolated point keeps the current limit and still results in the defined torque. Therefore, the $i_{d,ll}/i_{q,ll}$-point must be shifted along its corresponding flux ellipse towards lower current amplitudes. This operation is conducted using the current vector $\boldsymbol{i}_{ll}$ with amplitude $|\boldsymbol{i}_{ll}|$ and angle $\angle\boldsymbol{i}_{ll}$. The correct current amplitude $|\boldsymbol{i}_{ll}|$ for the lower limit torque controller from the upper limit current amplitude $|\boldsymbol{i}_{ul}|$ can be calculated with:

$$|\boldsymbol{i}_{ll}| = i_{max} + b\,(i_{max} - |\boldsymbol{i}_{ul}|) \tag{11}$$

$$b = \frac{i_{sc,ll} - i_{sc,ind}}{i_{sc,ind} - i_{sc,ul}}. \tag{12}$$

With this current amplitude, the interpolated current will keep the current limit i_{max}. To gain the correct current angle $\angle\boldsymbol{i}_{ll}$ for the shift along the flux ellipse an additional LUT is needed:

$$\angle\boldsymbol{i}_{ll} = \mathrm{f}(|\boldsymbol{i}_{ll}|, \psi_{lim}). \tag{13}$$

This LUT can be calculated offline with the other LUTs introduced in Section 2 from the flux information $\psi(i_d, i_q)$ for the lower limit sample.

3.6 Extension 3: Adaption of upper limit current point

A third area with significant torque errors is at the lower MTPF line, where the operation is limited by voltage limit but not by current limit. It

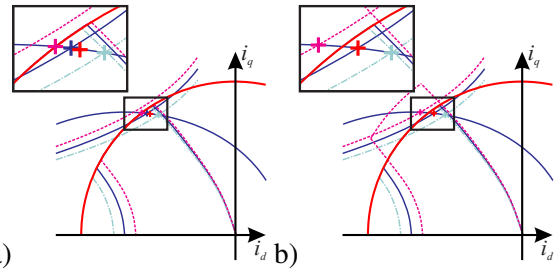

Figure 7: Extension 2: a) lower limit torque controller gets limited by the current limit, leading to significant torque error. b) extension of the LUTs for lower limit torque controller leads to correct interpolated current point.

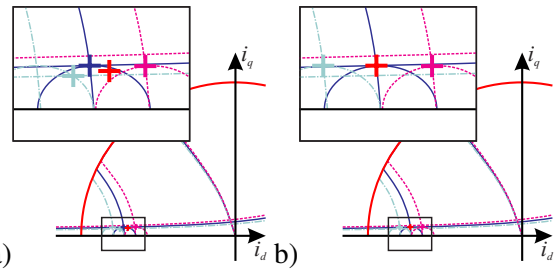

Figure 8: Extension 3: a) no intersection of torque command isoline and limiting flux isoline can be found at lower MTPF and current point at maximum reachable torque is chosen. Interpolation based on this point leads to torque error. b) Adaption of upper limit current point by modification of its torque command.

is marked by number 2 Fig. 5b. It is related to the discussion in Section 3.5 – again the lower limit torque controller reaches an operation limit while the upper and especially the reference machine are not restricted. Here, a modification of the upper limit torque controller is expedient. In Fig. 8a, the effective limiting flux ellipse of the characteristics of the reference machine is shown (blue solid line). The ellipses of lower limit and upper limit are the respective ones that are implemented in the corresponding torque controller. The lines in parallel to the d-axis represent the three torque isolines of commanded torque T^*. The intersection point of the flux ellipses and their corresponding torque isoline is the i_d/i_q operation point of choice. For the upper limit torque controller, this point can be found. For the lower limit torque controller, there is no intersection point and the point giving the maximum torque is chosen. Interpolating these two points leads to a interpolated point that produces less torque than the reference machine is capable of.

The solution is to increase the torque command for the upper limit torque controller T^*_{ul} by the difference between commanded T^*_{ll} and limited

torque $T_{lim,ll}$ of the lower limit torque controller:

$$T^*_{ul,new} = T^*_{ul} + (T^*_{ll} - T_{lim,ll}). \quad (14)$$

$T_{lim,ll}$ therein is the maximum torque the lower limit torque controller can achieve at the given speed. The upper limit torque controller is then commanded with this new value $T^*_{ul,new}$, leading to a correct i_d/i_q-point for the reference machine. The operation is visualized in Fig. 8b.

3.7 Extended Parallel Torque Compensation (PTC)

Integrating the extensions 1-3 into the sPTC structure shown in Fig. 1b finally leads to the Parallel Torque Compensation (PTC) structure in Fig. 1c. The commanded torque T^* is modified according to Section 3.4 before it is fed into the upper and lower torque controller. The LUTs in the lower torque controller are extended to a higher current limit according to Section 3.5. Finally the current calculated by the upper torque controller is treated according to Section 3.6 to optimize torque accuracy at the lower MTPF line. Using this structure, the torque error can be significantly reduced. Fig. 5c shows the torque accuracy that can be reached with PTC in simulation, the maximum torque error can be reduced to 0.21 % . In Section 4 the effectiveness of the torque compensation with PTC in measurement is demonstrated.
The PTC can not only be used for permanent magnet flux deviation, it can also be applied to other sources of deviations in the machine. As shown in Section 3.1, the air gap width in the machine is the second important influence factor on torque accuracy. An PTC for the exclusive compensation of an air gap deviation can be set up in exact the same way as it is done for the permanent magnet deviation.

3.8 Implementation of PTC for deviations in permanent magnet and air gap

Given this, it is desirable to find a compensation strategy that can compensate for both, permanent magnet flux deviation and deviations of the air gap width. One option can be derived from PTC: The PTC-structure in Fig. 1c can again be doubled gaining the structure in Fig. 9a, adding up to the 2-dimensional 2D-PTC. With that, four parallel torque controllers calculate their respective i_d/i_q-combination. As depicted in Fig. 9b, the LUTs of each torque controller contain two effects, one permanent magnet and one air gap deviation. The currents calculated are then interpolated with a two-dimensional linear interpolation method.

Two out of the four torque controllers are clearly defined: The one that represents the *upper limit* for permanent magnet flux and the *upper limit* for air gap will be the uppermost limit controller. The one representing the *lower limit* for permanent magnet flux and the *lower limit* for air gap will be the undermost limit controller. The i_d/i_q-points calculated by these controllers can be treated as described for PTC by the extensions in Sections 3.4-3.6. The remaining two torque controllers contain contrary effects: One represents *lower limit* for permanent magnet flux and the *upper limit* for air gap and the other *upper limit* for permanent magnet flux and the *lower limit* for air gap. Therefore, each of them has one effect that increases and one that decreases torque. Therefore, their currents are not specifically treated, which leads to minor torque error in certain operation points. Fig. 10 displays simulation results of the 2D-PTC.

In Fig. 10a, the torque error of the uppermost limit sample machine with $5\,\%$ deviation in its permanent magnets and $30\,\%$ deviation in the air gap driven with a conventional torque controller based on reference data is shown. A maximum deviation of over $10\,\%$ is visible.

In contrast, Fig. 10b shows the error resulting from 2D-PTC set up with characterizations of $\pm 5\,\%$ deviation in their permanent magnets and $\pm 30\,\%$ deviation in the air gap. Again, driving a limit sample machine with 2D-PTC leads to zero torque error as the currents can be determined exactly. The 2D-PTC is therefore applied to the reference machine (indicated by number 1 in Fig. 9b). With this, the interpolation targets into the center of the tolerance bands leading to a maximum torque error of $0.14\,\%$. Even for a scenario where the 2D-PTC is applied to an individual machine with a magnet deviation of $2\,\%$ combined with an air gap deviation of $25\,\%$ (indicated by number 2 in Fig. 9b), the torque error is at a maximum of $0.26\,\%$ which is still very good.

4 Experimental results

To prove the simulation results, two machines with intentional deviation of more than $10\,\%$ of their magnets' remanence field density are investigated. The machine with the weaker magnets is the *lower limit sample* and the one with the stronger magnets is the *upper limit sample*. At first, the lower limit sample is considered as reference machine. The LUTs in the torque controller used in the inverter are fitted to the reference (lower limit) machines characteristic. All results are gained at a rotor temperature of $60\,°C$ if not stated differently. Driving this reference machine at the dyno with its corresponding LUTs leads to the torque accuracy shown in Fig. 11a.

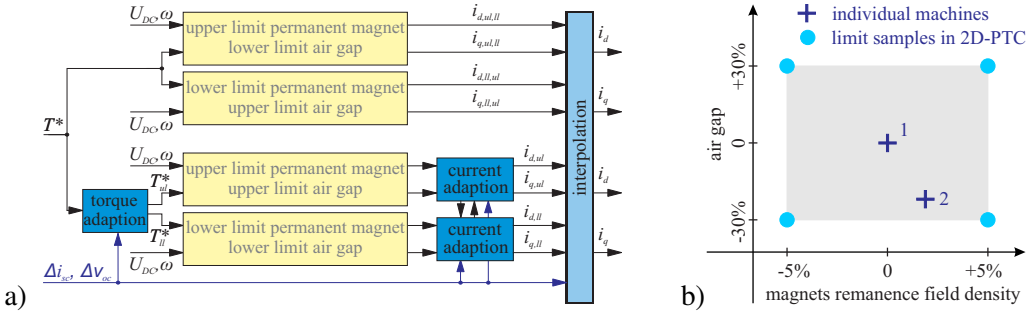

Figure 9: 2D-PTC: a) the structure contains four parallel torque controllers, each delivering one pair of i_d/i_q-currents. b) each set of LUTs in the controllers contain two limit samples properties – one of permanent magnet flux and air gap.

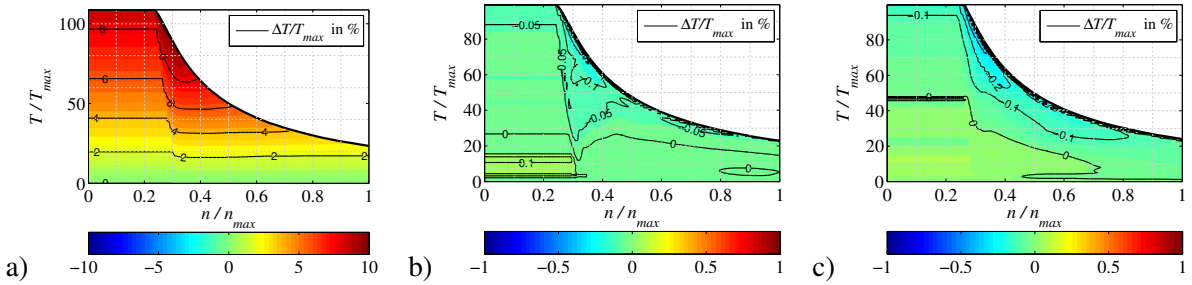

Figure 10: Torque accuracy for individual machines with deviations in their magnets *and* air gap at the same time: a) without compensation, b) with 2D-PTC for a machine in the center (point 1 in 9b) and c) at a magnet deviation of 2 % combined with a air gap deviation of 25 % (point 2 in 9b).

The torque error is defined as

$$\Delta T = T_{meas} - T^*. \tag{15}$$

Here, a maximum torque error of $\Delta T/T_{max} = 1.4\,\%$ is visible, which is considered as sufficiently precise for a standard torque controller.
To set up the PTC algorithm, only the characteristics of the reference machine are used. Based on the investigations discussed in Section 3.1 characteristics for both, upper and lower limit samples can be derived. This approach would be taken if only the reference machine was available during development. With the parallel torque controllers of PTC, again the reference machine is driven. All current and voltage limits are kept and the achieved torque accuracy (shown in Fig. 11b) is the same as in Fig. 11a within the scope of measurement accuracy. This proves the simulation results of Section 3.7 and therefore the correct functionality of PTC in measurement.

4.1 Compensation of temperature influence

The permanent magnets of the machine are significantly influenced by temperature. By measuring the open-circuit voltage at different rotor temperatures a temperature coefficient for the permanent magnets of

$$\alpha_{PM} = -0.1\,\%\mathrm{K}^{-1} \tag{16}$$

could be found. It is consistent to literature values, i.e. in [9]. As this coefficient influences the magnets' remanence field density, the effects are the same as for the magnets production tolerances.
To prove the influence, the reference machine is driven with its corresponding torque control LUTs. Running the machine at 60 °C gives the torque accuracy shown in Fig. 11a. Driving the machine at a rotor temperature of 35 °C leads to a maximum torque error of 3.0 % (Fig. 12a). Using the temperature coefficient and PTC this can be reduced to a maximum of 1.6 % (Fig. 12b), which only slightly worse than the reference at 60 °C. This is the torque error for a temperature deviation of $\Delta\vartheta = 25\,\mathrm{K}$. Assuming the temperature range for automotive machines of −40 °C to 120 °C, maximum temperature deviations and corresponding torque errors are even higher.

4.2 Compensation of production tolerance

Now, the characteristics of the upper limit sample are used as the reference. Still, the lower limit sample is driven at the dyno. For a first test run,

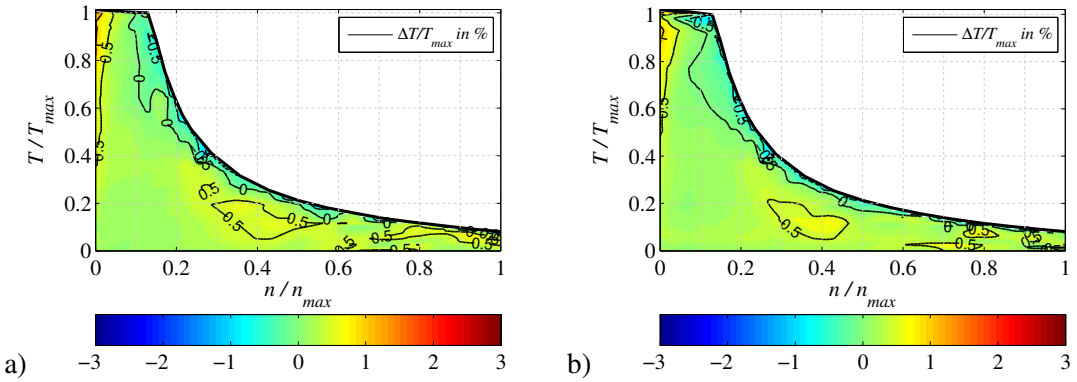

Figure 11: The reference machine is driven a) with conventional torque controller b) with PTC

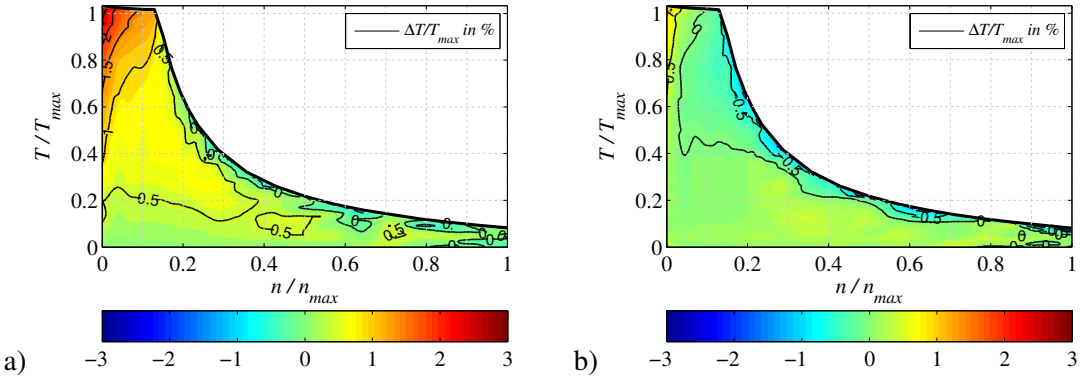

Figure 12: The reference machine is driven at a rotor temperature reduced by $\Delta\vartheta = 25\,K$. a) if no compensation is applied, torque accuracy is reduced. b) using PTC, torque accuracy can be restored.

the LUTs of the reference machine (upper limit) are used without PTC. As expected, a significant torque error of $\Delta T/T_{max} = -12\,\%$ can be seen in Fig. 13a. To use PTC, the measurements of short-circuit current as well as open-circuit voltage for both reference ($i_{sc,ref}$ and $v_{oc,ref}$) and lower limit sample machine ($i_{sc,ll}$ and $v_{oc,ll}$) are taken. With the ratios $i_{sc,ll}/i_{sc,ref} = 0.86$, $v_{oc,ll}/v_{oc,ref} = 0.87$ and $L_q/L_d = 0.66$, as well as the $\Delta i_{sc} = -0.16\,i_{sc,ref}$ for this machine, the equations in Section 3.2 can be used to set up PTC correctly. With this setup the maximum torque error can be reduced from -12 % to a maximum of about -2 % (Fig. 13b).

4.3 Maximum torque available

To evaluate the impact of magnets' remanence field density on systems maximum torque, six different setups are used and the results are shown in Fig. 14. The definition of which machines characteristics are used as reference and to generate the LUT for the torque controller and for PTC are defined according to each setup:

- "ll ref, ctrl: ll": The lower limit sample is driven with its affiliated LUTs. This is the setup in Fig. 11a.
- "ll uncomp, ctrl: ul": The lower limit sample is on the dyno, driven with LUTs of the upper limit sample. This is the setup also used in Fig. 13a.
- "ll comp, ctrl: ul-PTC": The lower limit sample is on the dyno, driven with PTC containing LUTs of the upper limit sample. This is the setup in Fig. 13b.
- "ul ref, ctrl: ul": The upper limit sample is driven on the dyno and the LUTs in the torque controller used in the inverter are fitted to its machines characteristic.
- "ul uncomp, ctrl: ll": The upper limit sample is on the dyno, driven with LUTs of the lower limit sample.
- "ul comp, ctrl: ll-PTC": The upper limit sample is on the dyno, driven with PTC containing LUTs of the lower limit sample.

In Fig. 14, a torque exceeding maximum torque is commanded to gain the maximum torque curve.
The setups "ul ref, ctrl: ul" and "ll ref, ctrl: ll" give the absolute maximum torque for the machines, as using the affiliated LUTs for each machine will always lead to the optimum control

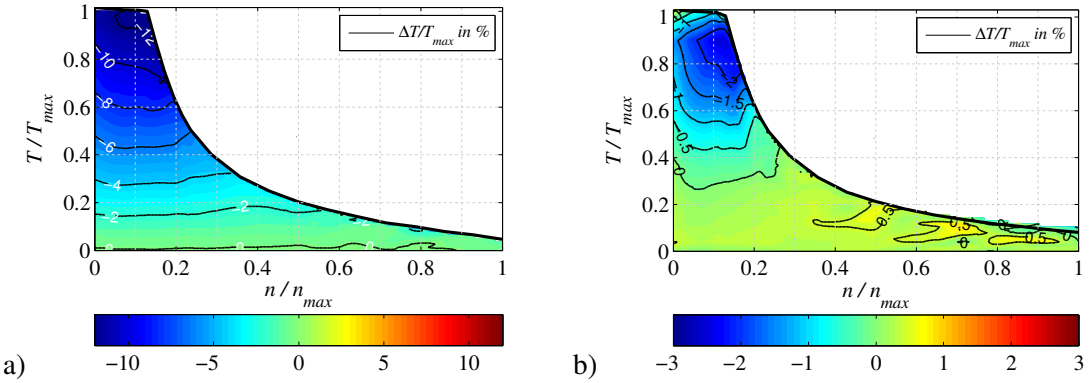

Figure 13: Torque errors measured at the dyno can be significantly reduced. The error is shown in a torque-speed-map a) without and b) with PTC.

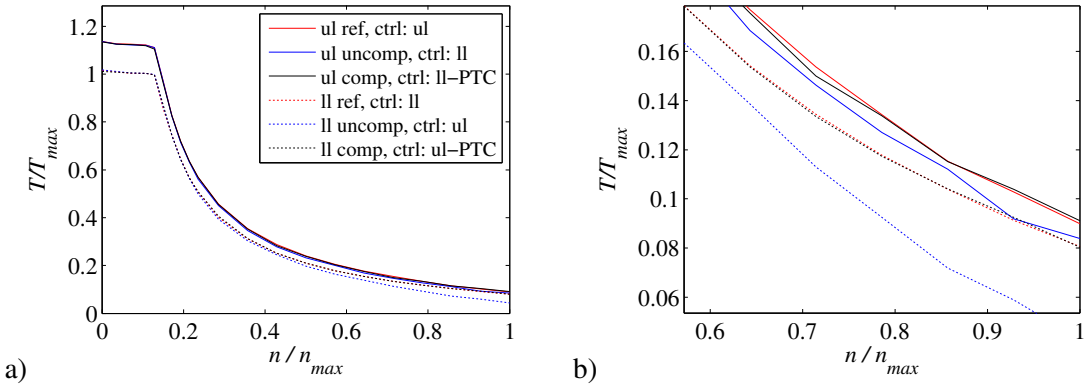

Figure 14: Comparison of the achieved torque at maximum torque command for each speed and different setups. a) full torque-speed-range, b) zoomed view for a).

strategy according to Section 2. Here, one important result can be seen: Driven with optimum control, the upper limit sample is always producing the higher maximum torque.

The setups “ul uncomp, ctrl: ll” and “ll uncomp, ctrl: ul” in Fig. 14 display the impact of a sub-optimal control for the limit sample machines at their maximum torque line. As the torque controller always stays within the area enclosed by the MTPC and MTPF lines, it will give operation points on the MTPF line for maximum torque command. To understand the effects, Fig. 2b can be considered: For “ul uncomp, ctrl: ll”, the machine is the upper limit while the MTPF line in the controller belongs to the lower limit. The MTPF line therefore is too far right for the machine, the real maximum torque cannot be reached within the allowed operation area. This is demonstrated in Fig. 14, as the available torque is slightly lower compared to the optimum controller. For “ll uncomp, ctrl: ul”, the machine is the lower limit while the LUTs and therewith the MTPF line in the controller belong to the upper limit sample. Here, the sub-optimal controller has a large negative impact. At this setup, the MTPF line is too far left and with maximum torque command, the absolute i_d-current fed into the machine is too high. The additional i_d-current actually *lowers* the torque instead of increasing it. Therefore, commanding a little less torque than the maximum leads to a higher torque than commanding the actual maximum – and the achieved torque at the maximum torque command is reduced. With this control and the investigated machines, the torque at maximum torque command of the lower limit sample – that is already reduced since it is the *lower* limit – is even *halved*.

As can be seen in Fig. 14, with PTC the exact same maximum torque lines as with the affiliated LUTs are be reached. PTC ensures optimum control for individual deviating machines.

5 Conclusion

The knowledge about the impact of the tolerances is used to adapt the flux linkage tables of a reference machine with nominal parameters. An implementation of the concept for the inverter software is presented. A parallel torque compensation (PTC) strategy is applied to gain optimum i_d/i_q-currents for a given torque command. The difference between system operation with

and without compensation is shown. Using the method in simulation on a machine with a permanent magnet flux deviation of 5 % shows a significant reduction of torque error from 4 % to 0.4 % with respect to maximum torque. The method is applied at a test bench for a pair of exemplary machines, where the predicted increase of torque accuracy is confirmed, reducing the torque error from 12 % to 2 %. This can not only be applied for production tolerance, temperature effects can be treated, too. Without compensation, not only torque accuracy is involved but also the achieved torque decreases significantly at maximum torque command. This decrease can be revoked using PTC.

References

[1] M. Balluff, H. Naumoski, and K. Hameyer, "Sensitivity analysis on tolerance induced torque fluctuation of a synchronous machine," in *Electric Drives Production Conference and Exhibition*, 2016.

[2] A. S. Babel, S. N. Foster, J. G. Cintron-Rivera, and E. G. Strangas, "Parametric sensitivity in the analysis and control of permanent magnet synchronous machines," in *International Conference on Electrical Machines (ICEM)*, 2012.

[3] H. Khreis, A. Deflorio, K. Voelz, and B. Schmuelling, "Sensitivity analysis on electrical parameters for permanent magnet synchronous machine manufacturing tolerances in EV and HEV," in *IEEE Transportation Electrification Conference and Expo*, 2016.

[4] G. Ombach and J. Junak, "Design of PM brushless motor taking into account tolerances of mass production - six sigma design method," in *IEEE Industry Applications Annual Meeting*, 2007, pp. 2139–2146.

[5] M. Ott and J. Böcker, "Sensitivity analysis on production tolerances for electric drive systems in automotive application," in *European Conference on Power Electronics and Applications (EPE)*, 2016.

[6] D. Coupek, A. Gülec, A. Lechler, and A. Verl, "Selective rotor assembly using fuzzy logic in the production of electric drives," in *CIRP Conference on Intelligent Computation in Manufacturing Engineering (CIRP ICME)*, 2014.

[7] H. Khreis, A. Deflorio, and B. Schmuelling, "A novel online PMSM parameter identification method for electric and hybrid electric vehicles based on cluster technique," in *International Electric Machines & Drives Conference (IEMDC)*, 2015.

[8] G. Rang, J. Lim, K. Nam, H.-B. Ihm, and H.-G. Kim, "A MTPA control scheme for an IPM synchronous motor considering magnet flux variation caused by temperature," in *Applied Power Electronics Conference and Exposition (APEC)*, 2004.

[9] O. Wallscheid and J. Böcker, "Wirkungsgradoptimale Arbeitspunktsteuerung für einen permanenterregten Synchronmotor mit vergrabenen Magneten unter Berücksichtigung von Temperatureinflüssen (in German)," in *Internationaler ETG-Kongress*, 2013.

[10] M. Meyer and J. Böcker, "Optimum control for interior permanent magnet synchronous motors (IPMSM) in constant torque and flux weakening range," in *Power Electronics and Motion Control Conference (EPE-PEMC)*, 2006.

Authors

Markus Ott studied mechatronic engineering at the FAU Erlangen-Nuremberg, Germany, from 2008-2014. Since 2014 he is working as doctoral candidate at Daimler AG in Sindelfingen. In his work he focuses on the detection and compensation of the effect of tolerances in the electrical drive system.

Alexander Beckmann studied electrical engineering at the RWTH Aachen, Germany, from 2011 - 2016. He worked at Daimler AG in Sindelfingen for his masters-thesis in the field of electric machine control.

Prof. Dr.-Ing. Joachim Böcker studied electrical engineering at the Technical University of Berlin and received his doctorate degree there in 1988. He worked at the AEG Research Institute, later Daimler Research and Development, in Berlin from 1988-2001. Since 2003 he is professor for Power Electronics and Electrical Drives at the Paderborn University.